Journal of Environmental Chemical Engineering 11 (2023) 110813

Contents lists available at ScienceDirect

Journal of Environmental Chemical Engineering

journal homepage: www.elsevier.com/locate/jece

Inactivation of *E. coli* and *S. aureus* by novel binary clay/semiconductor photocatalytic macrocomposites under UVA and sunlight irradiation

Silvio Aguilar [a,b,*], Briggitte Guerrero [a], Ángel Benítez [a], Daniel R. Ramos [b], J. Arturo Santaballa [b], Moisés Canle [b], Daniel Rosado [a,c], Javier Moreno-Andrés [d,**]

[a] GIMA Group, Department of Chemistry, Faculty of Exact and Natural Sciences, Universidad Técnica Particular de Loja, 11 01 608 Loja, Ecuador
[b] React! Group, Department of Chemistry, Faculty of Sciences & CICA, Universidade da Coruña, E-15071 A Coruña, Spain
[c] Department of Hydrology and Water Resources Management, Institute for Natural Resource Conservation, Kiel University, 24118 Kiel, Germany
[d] Department of Environmental Technologies, Faculty of Marine and Environmental Sciences. INMAR-Marine Research Institute, CEI-MAR-International Campus of Excellence of the Sea, University of Cadiz, Spain

ARTICLE INFO

Editor: Despo Fatta-Kassinos

Keywords:
Heterogeneous photocatalysis
Semiconductor-clay macrocomposites
Photocatalytic disinfection
Solar disinfection
Ecuadorian clay

ABSTRACT

The disinfection efficiency of several novel photocatalytic macrocomposites made of Ecuadorian clay mixed with two semiconductor materials (TiO_2, ZnO) has been evaluated with *Staphylococcus aureus* and *Escherichia coli* as target bacteria. They have been tested under two irradiation sources (UVA lamp and sunlight) in different configurations. Two different semiconductor/clay ratios (60/40 and 80/20) were tested at 10–20 $g{\cdot}L^{-1}$ (with UVA) and 20–40 $g{\cdot}L^{-1}$ (with sunlight) composite loadings. With the presence of the photocatalyst, a four- to five-fold increase in the inactivation rate by UVA was observed with respect to single UVA inactivation, while the performance with sunlight reaches up to six-fold. The particular effect of nature, ratio and loading on the inactivation kinetics depends on the specific bacterial species tested. In this case, the inactivation of *S. aureus* was faster in comparison with *E. coli*, probably due to the interaction between bacteria and the catalytic material and the associated ζ-potential. In general, the 80% ZnO composites at maximum loading show the highest efficiency, comparable to that of nanosized semiconductors. The ability of these composites to maintain a high disinfection efficiency after three uses, together with their low cost and ease of recovery, make these composites an attractive option for wider use in water disinfection facilities.

1. Introduction

Worldwide, over 2 billion people use drinking water sources containing, to some extent, faecal contamination. Unsafe drinking water causes an estimated 485,000 deaths per year from diarrhoea alone, most of them in developing countries [1]. Lack of sufficient sanitation services coupled with rapid urbanisation, population growth and poor infrastructure promote the spread of disease, generating significant health and environmental concerns [2,3]. Consequently, the United Nations included "Ensure availability and sustainable management of water and sanitation for all" as one of the 17 Sustainable Development Goals to be achieved by 2030 [4].

Solar disinfection (SODIS) is a recognized water treatment method in locations where access to safe drinking water is problematic [5]. However, SODIS effectiveness generally depends on meteorological and climatological factors according to latitude location [6]. Sunlight can also drive advanced oxidation processes (AOPs), which lead to oxidation of organic molecules and microorganisms inactivation. Therefore, they have a great potential for water treatment. Hydroxyl radicals ($HO^{\bullet}$) generated in AOPs are the strongest oxidising species in aqueous solution; they are short-lived, easily produced, electrophilic, ubiquitous in nature, highly reactive and practically non-selective [7]. Heterogeneous photocatalysis is one of the most promising techniques among AOPs. A major drawback of light-driven AOPs for water treatment is the high cost of artificial photon generation, especially when large volumes of water are involved [8]. Therefore, sunlight-driven AOPs have attracted much interest among researchers, particularly considering that sunlight is clean, safe, very abundant and renewable [9,10]. Nearly $3{\cdot}10^{24}$ J of

* Corresponding author at: GIMA Group, Department of Chemistry, Faculty of Exact and Natural Sciences, Universidad Técnica Particular de Loja, 11 01 608 Loja, Ecuador.
** Corresponding author.
E-mail addresses: sdaguilar@utpl.edu.ec, david.aguilar1@udc.es (S. Aguilar), javier.moreno@uca.es (J. Moreno-Andrés).

https://doi.org/10.1016/j.jece.2023.110813
Received 2 May 2023; Received in revised form 11 August 2023; Accepted 19 August 2023
Available online 22 August 2023

sunlight energy reach Earth's surface per year, approximately ten thousand times as much as the annual gross energy consumption of humanity worldwide [11,12].

The effectiveness of catalysts used in heterogeneous photocatalysis is highly dependent on the quality and properties of the stand-alone, composite or combination of chosen catalysts [13]. The combination of the disinfection capacity of UV radiation with the excellent antimicrobial properties of some nanosized semiconductors, such as TiO_2 and ZnO, has been studied and high disinfection rates were achieved [14–17]. However, some relevant problems remain to be solved: the difficulty and high cost of their removal from treated water to be reused, the loss of nanoparticles that may end up in the environment and the drop in efficiency when recycled [18,19].

Supported nanosized semiconductors can prevent the release of nanoparticles into the environment and facilitate their separation and reuse. Therefore, it is necessary to develop suitable supported catalysts [13]. Immobilisation techniques on appropriate supports, such as porous glass, activated charcoal, zeolites and kaolinite, improve some morphological, surface and adsorption properties [20,21]. Some studies report that immobilising semiconductors decreases their efficiency, as compared to the corresponding particulate form, mainly due to the reduction of the catalytic surface area [22]. This often requires the coupling of specific templates or surfactants by high-temperature treatment, where the regulation of the pore structure is difficult, resulting in higher preparation costs [23]. Moreover, this immobilisation is usually weak due to poor attachment of the catalyst to the support material, which results in a loss of activity in subsequent uses [24–26].

The immobilisation of TiO_2 and ZnO on the surface of various porous clay materials provides more catalytically active surface sites, reduces the agglomeration of nanoparticles, prevents the release of nanoparticles into the environment, and facilitates the separation of the photocatalysts and their reuse [27,28]. Thus, clay-based hybrid photocatalysts showed great potential for environmentally related applications due to some of their properties: abundance, low cost and environmental friendliness [11,29]. In addition, clays often show regularly arranged silica-alumina frameworks, and some studies report that the aluminium present in the clay, when mixed with TiO_2, delays the phase transition process from anatase to rutile during calcination, allowing the composites to be processed at higher temperatures to achieve higher hardness without loss of efficiency [13]. Besides, some clays produce a doping effect in the semiconductor, increasing its efficiency to levels higher than those of the pure semiconductor [30].

Ecuadorian clays have been used in adsorption and photocatalysis studies [31]. In previous research a newly clay-based photocatalyst was developed [32], currently under patent no. ES2916381. These composites have already been tested for the removal of phenol with UVA [32] and of several pollutants with sunlight [33]. However, reports on disinfection are scarce. Therefore, the aim of this study is to evaluate the disinfection efficiency of this novel photocatalytic composite prepared with an Ecuadorian clay and metal oxide semiconductors: TiO_2 or ZnO. Thus, the effects of the irradiation source (sunlight or UVA lamp), loading (concentration of the composite in water, $g{\cdot}L^{-1}$), and percentage of semiconductor in the material (%) have been addressed for the inactivation of two target bacteria: the gram-positive *Staphylococcus aureus* and the gram-negative *Escherichia coli*.

2. Materials and methods

2.1. Microbiological procedures

Staphylococcus aureus (*S. aureus*) and *Escherichia coli* (*E. coli*) have been selected as gram-positive and gram-negative bacterial representatives, respectively. Both bacteria are pathogenic to humans and, due to the existence of extensive previous research on them, have been selected as model organisms in this study [34–37].

Lyophilized commercial strains of *S. aureus* (ATCC 6538®) and *E. coli* (ATCC 25922®) were reactivated and cryogenically stored at −80 °C in 1 mL Eppendorf tubes with 900 μL of DIFCO nutrient broth (Becton, Dickinson and Company) and 100 μL of dimethyl sulfoxide (ACS, Fisher Chemical) [38,39]. Strains were activated by keeping them at room temperature (20–25 °C) for 5 min, and then vortexed for 2 min at 200 rpm. 100 μL were transferred to test tubes containing 10 mL of nutrient agar and incubated for 24–48 h at 37 °C in a Thermo Scientific incubator. To obtain the initial concentration for inactivation experiments (see Section 2.4.), bacteria were inoculated into test tubes containing 10 mL of sterile water using a 10 μL loop. The process was repeated until the turbidity reached 6 (*S. aureus*) or 5 (*E. coli*) on the McFarland scale, measured with a densitometer (model DEN-1, Grant Instruments). After standing for 5 min, the solutions obtained were diluted to 1000 mL with autoclaved 9 $g{\cdot}L^{-1}$ NaCl (ACS, Fischer Chemical) solution. During disinfection tests, the bacterial concentration was expressed as colony forming units (CFU) per mL. Accordingly, the explained procedure gave a concentration of approximately 10^6 $CFU{\cdot}mL^{-1}$.

After inactivation assays, the remaining CFU were quantified to assess the efficacy of the disinfection processes. Aliquots of 1 mL were taken at different exposure times. Depending on the expected bacterial concentration, the aliquots were either used directly or diluted with sterile buffered water (pH = 7.2, 1.25 $mL{\cdot}L^{-1}$ of 0.25 $mol{\cdot}L^{-1}$ KH_2PO_4 buffer -p.a., Merck-), and seeded in Petri dishes in triplicate. Baird Parker agar for *S. aureus* and MacConkey agar for *E. coli* (both from Becton Dickinson, BD) were used as solid media in Petri dishes. After 48 h of incubation at 37 °C in a Thermo Scientific incubator, CFU were quantified with a colony counter, considering a minimum value of 2 $CFU{\cdot}mL^{-1}$. All microbiological procedures were carried out in a class II, laminar flow biosafety cabinet.

2.2. Preparation of the photocatalytic composites

The photocatalysts employed in this study have been prepared according to a previous study [32]. Briefly, they consist in macrocomposites with photocatalytic activity composed of a natural clay and a semiconductor (TiO_2 or ZnO), homogeneously dispersed throughout the piece. The photocatalyst was prepared as follows: a natural Ecuadorian clay was thoroughly mixed with the semiconductor, both in powder form, in the desired mass ratio; distilled water was added dropwise to this homogeneous mixture with gentle stirring until a firm, plastic paste was obtained, which was extruded into long cylinders using a syringe with a 2.1 mm inner diameter tip; the cylinders were dried in an oven at 90 °C for 12 h, broken into small pellets about 0.5 cm long, and then calcined at 600 °C for 3 h with a heating ramp of 5 $°C{\cdot}min^{-1}$; after cooling, they were rinsed with distilled water and dried again at 90 °C for 12 h. These pellet-shaped composites were prepared with clay and either TiO_2 or ZnO in mass ratios of 40/60 and 20/80.

A detailed description of their preparation and physicochemical characterisation can be found in [32]. Also, previous tests have been performed for the photodegradation of chemical pollutants with artificial UV radiation [32] and sunlight [33].

2.3. Characterization

The clay used for the preparation of the composites (named P_1M_2) was extracted from the Miocene sedimentary basin of Loja in southern Ecuador. It was used directly after drying at 90 °C, grinding and sieving (250 μm mesh). This clay has been extensively characterised by analysing its chemical composition, organic matter content, mineral phases, particle size, density, specific surface area and pore size [32]. This clay has been mixed with Degussa Aeroxide TiO_2-P25, hereafter referred to simply as TiO_2, or with Sigma-Aldrich ZnO (ReagentPlus®, 99.9%) to produce the photocatalytic material. The homogeneity of these pellets has been confirmed by field emission scanning electron microscopy coupled to energy dispersive X-ray spectroscopy (FESEM/EDX), and the effect of the calcination step on the anatase to rutile phase transition has

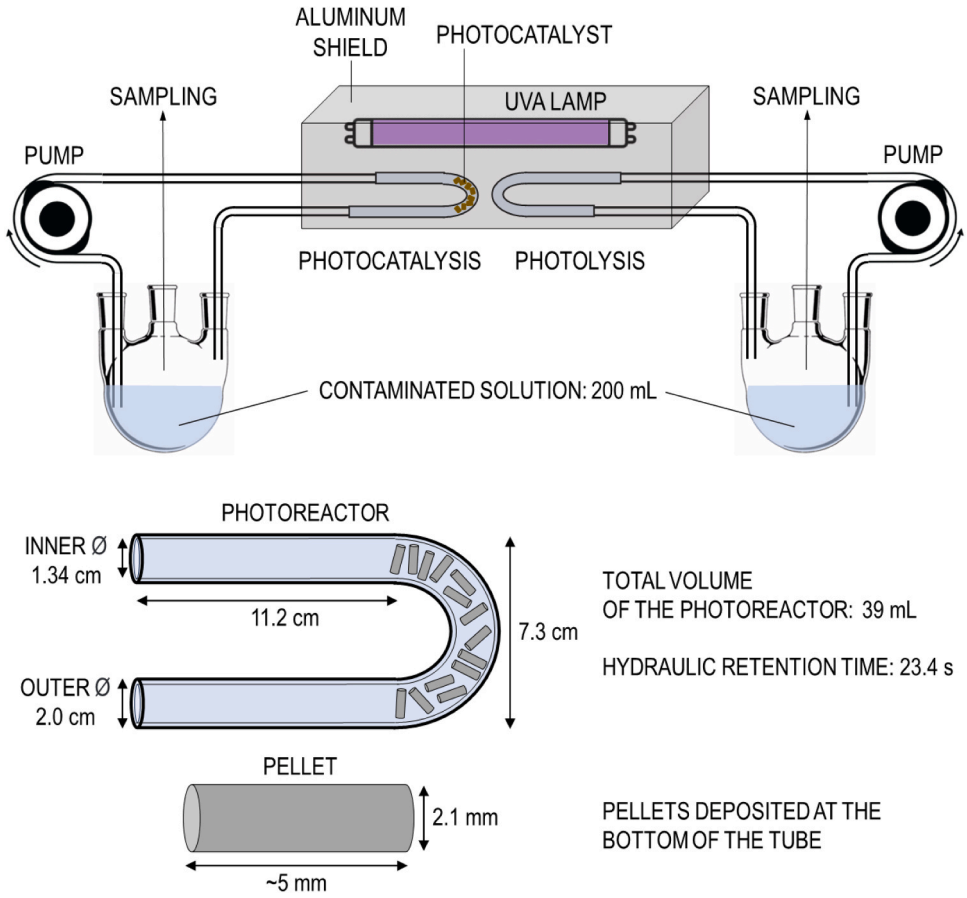

Fig. 1. Schematic image of the photoreactor used in the experiments with the UVA lamp.

been determined by X-ray diffraction [32].

In the present work, in addition to the above, the leaching of the photocatalytic composite was studied by keeping 20 g·L^{-1} of 80% pellets in water for 72 h, *i.e.* much longer than in the inactivation experiments (see below). The liquid was then analysed by inductively coupled plasma atomic emission spectroscopy (ICP-AES) using a Perkin Elmer Optima 8000 instrument to quantify the elements of interest. The ζ-potential of the starting materials was also measured at natural pH in a Zetasizer Nano ZS analyser (Malvern Panalytical), and the ZnO mineral phases were determined by X-ray diffraction in a D8 Advance ECO, Bruker device.

2.4. Inactivation experiments

Two different UV sources have been used to irradiate the macro-composites produced, *i.e.,* a UVA lamp and natural sunlight. Two clay/semiconductor ratios, *i.e.* the percentage of semiconductor (TiO_2 or ZnO) on the total weight: 60 or 80% has been contemplated for experimentation. In addition, two composite loadings, expressed as the concentration in g·L^{-1} of photocatalytic material in the inoculated solution, were tested to study the inactivation of *S. aureus* and *E. coli*.

2.4.1. UVA lamp tests

The photoreactor used for UVA experiments is depicted in Fig. 1. It allows two experiments to be carried out simultaneously. Each half consisted of a 250 mL round-bottom three-necked flask into which 200 mL of the inoculated solution was poured and a peristaltic pump propelled this water at a flow rate of 100 mL·min^{-1} into a U-shaped quartz tube, where the catalytic pellets were placed, obtaining a catalyst loading of 10 or 20 g·L^{-1}. The composite pellets are large enough and of sufficient density (> 3 g·mL^{-1}) to remain deposited at the bottom under slow laminar flow. The total reactor volume was 39 mL, corresponding to a hydraulic retention time (HRT) of 23.4 s.

This system was illuminated with a 50 W UVA lamp with peak emission at 365 nm (UVP Mineralight UVL-225D P/N 95–0190–01). The average incident radiation was determined as 18.95 mW·cm^{-2} with a PCE-UV34 UVA-UVB radiometer (290–390 nm). At the required exposure times, samples were taken in duplicate.

2.4.2. Solar tests

The inactivation efficiency of solar radiation was evaluated in batch conditions, but higher composite concentrations were employed, 20 and 40 g·L^{-1}, based on the UVA results. The experiments were carried out under direct solar radiation at the Universidad Particular de Loja, Loja, Ecuador (3° 59′ 11′’ S, 79° 11′ 53′’ W). For each experiment, 100 mL of the inoculated solution was poured into a 250 mL borosilicate glass Erlenmeyer flask, with catalytic pellets deposited at the bottom, and was

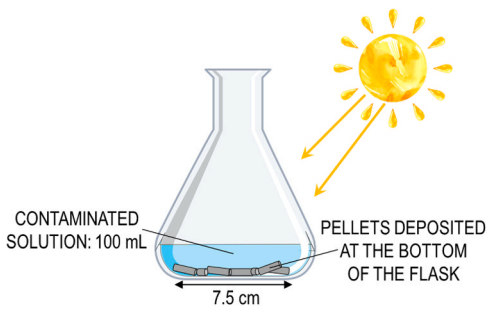

Fig. 2. Schematic image of the photoreactor used in the solar experiments and in the dark.

exposed to direct sunlight (Fig. 2). Duplicate samples were taken at the required times throughout the experiment. The average incident UV radiation (7.2 $mW \cdot cm^{-2}$) was measured with the same radiometer placed next to the Erlenmeyer flasks during the experiments. Experiments were also carried out in the dark with 20 $g \cdot L^{-1}$ composite using the same batch reactors.

2.4.3. Recovery and reuse

The pellets employed were reused 3 times to evaluate their stability and reuse efficiency. For this purpose, the composites were recovered after each inactivation, rinsed with distilled water and dried at 90 °C for 12 h. The corresponding experiment was then repeated under the same conditions as described in the previous sections.

2.5. Data treatment

The inactivation of bacteria in each experimental test was evaluated as the logarithm of the ratio of the number of bacteria after an exposure time t (N_t) to the initial number (N_0), *i.e.*, log (N_t/N_0). Bacterial concentration is stated as $CFU \cdot mL^{-1}$, using the mean value ± the standard deviation calculated from the duplicates. The disinfection performance was quantified using a first order kinetic equation (Eq. 1).

$$N_t = N_0 \cdot e^{-k_{obs} \cdot t} \quad (1)$$

The experimental data were fitted using a log-linear approach with direct weighting of the data standard deviation, to calculate the pseudo-first order rate constant, k_{obs} (min^{-1}), and the standard error (S.E.). The validity of this approach was assessed by the values of the coefficient of determination (R^2) and the root mean square error (RMSE). Unacceptably inaccurate values were obtained only for some very fast sunlight-driven reactions, for which very few data were obtained. The maximum inactivation level detected is between 6.08 and 7.31 log-removal values and 5.69–6.69 log-removal values for *E. coli* and *S. aureus* respectively.

3. Results and discussion

3.1. Properties of the raw materials and the photocatalytic composites

The starting materials used to prepare the composites have been previously characterised [32] and some additional analyses have been carried out in the present study. These data are summarised in Table 1.

According to the leaching tests, the photocatalytic composites prepared with TiO_2 are very stable; the total amount of Ti leached from the photocatalytic pellets after 72 h in contact with water was only 3.16 $\mu g \cdot L^{-1}$. In the case of the ZnO pellets, a much higher value was found for Zn (2.86 $mg \cdot L^{-1}$), which indicates some instability in this case. Nevertheless, both values comply with EU [40] and US EPA [41] drinking water regulations, which do not set limits for these two metals due to their low toxicity. In addition, these low measured concentrations rule out any significant photocatalytic activity of suspended semiconductor particles under the conditions used in this study.

3.2. UVA lamp tests

The inactivation profiles of *S. aureus* and *E. coli* obtained with the UVA lamp are displayed in Fig. 3 and the kinetic values listed in Table 2. Negligible inactivation of these microorganisms was obtained in the dark tests, which are also shown in Fig. 3 for comparison.

A slow inactivation of both bacteria by single UVA irradiation was observed (Fig. 3), with only up to a 2 log reduction of *E. coli* being achieved after 300 min exposure, and a 1.37 log reduction of *S. aureus* after 180 min. When subjected to UVA, cells may experience DNA and oxidative damage due to the direct action of light [42]. Previous research suggests that components involved in the metabolic cycle, such as lipids, certain proteins, and reactive oxygen species (ROS) scavengers, like catalases or superoxide dismutase, are particularly affected by UVA radiation. In addition, singlet oxygen could potentially contribute to this damage [43]. However, it has previously been found that UVA radiation has little effect on bacteria under these conditions and that significant germicidal effects require much higher exposure times and UVA doses than those tested in our study, with similar effects on different types of microorganisms [44,45]. In the presence of the photocatalytic composites, the inactivation of bacteria is significantly enhanced (Fig. 3 and Table 2), with rates 2.0–6.5 times that of UVA inactivation for *E.coli*, and 4.6–11.5 times for *S. aureus*. In addition, some interesting differences can be observed between both bacterial species tested and the photocatalysts used.

In the photocatalytic disinfection mediated by TiO_2 composites (Fig. 3A, B), *S. aureus* is inactivated more effectively than *E. coli*, as follows from the kinetic constants obtained for *S. aureus*, which are twice those of the latter (Table 2). In addition, a 4 log reduction in the concentration of *E. coli* was achieved in 2–4 h, while only 60–100 min were required for the same reduction with the other bacteria. The composites with 80% TiO_2 have a higher catalytic activity, 36% on average, than the

Table 1
Chemical composition (compounds obtained in a concentration higher than 0.01% by weight), mineral phases observed, and physical properties measured for the starting raw materials: density, average particle size, and ζ-potential.

	Chemical composition (%)								
P_1M_2 clay[a]	SiO_2	Al_2O_3	Fe_2O_3	SO_3	K_2O	MgO	CaO	Na_2O	TiO_2
	67.5	15.6	6.4	3.1	2.8	1.9	0.96	0.72	0.48
	P_2O_5	Cl	BaO	MnO	ZrO_2	SrO	ZnO	CuO	Rb_2O
	0.15	0.12	0.083	0.031	0.016	0.014	0.013	0.013	0.012
TiO_2-P25[a]	TiO_2	Cl	CuO						
	99.8	0.12	0.017						
ZnO[b]	ZnO								
	99.9								

	Mineral phases					
P_1M_2 clay[c]	Quartz	Albite	Olivine	Muscovite	Anorthite	Calcite
TiO_2-P25[a]	Anatase	Rutile				
ZnO[d]	Wurzite	Sphalerite				

	Density ($g \cdot mL^{-1}$)	Mean particle size (μm)	ζ-potential (mV)
P_1M_2 clay	2.82[a]	17.00[c]	–9.20[d]
TiO_2-P25	4.38[a]	6.02[c]	31.7[d]
ZnO	5.68[b]	0.34[b]	27.4[d]

[a] Ref. [32];
[b] According to the manufacturer;
[c] Determined from the data in [32];
[d] This work.

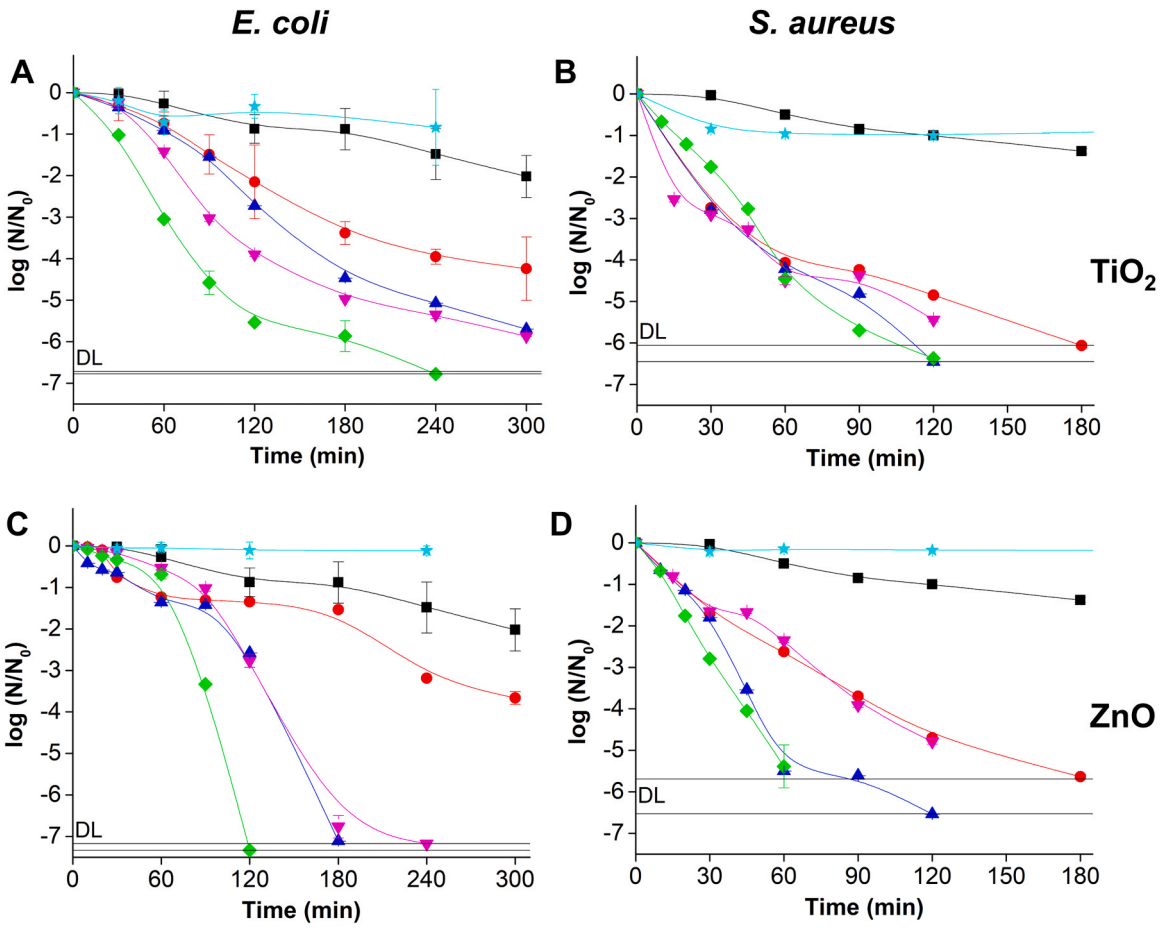

Fig. 3. UVA inactivation of *E. coli* (A, C) and *S. aureus* (B, D) with TiO_2 (A, B) and ZnO (C, D) photocatalysts as a function of composite loading and semiconductor percentage: dark test with 20 g·L^{-1} of 80% pellets (—★—), single UVA radiation (—■—), and photocatalysis with 10 g·L^{-1} of 60% (—●—), 10 g·L^{-1} of 80% (—▲—), 20 g·L^{-1} of 60% (—▼—), and 20 g·L^{-1} of 80% (—◆—) pellets. Natural pH, distilled water, T = 30 °C.

60% TiO_2 material, and the effect of loading on the disinfection rate is also evident: the experiments with 20 g·L^{-1} yielded rates about 50% faster than with half this loading. Interestingly, the disinfection rate does not increase linearly with the composite loading, which may be due to the fact that they shade each other in the reduced space of the reactor tube, and the illuminated surface area does not increase proportionally to the catalyst loading. Thus, the maximum inactivation efficiency was obtained when using 20 g·L^{-1} of 80% TiO_2 composite.

In the case of the experiments performed with ZnO composites, the inactivation profiles showed a partial-induction period of 60–90 min for the inactivation of *E. coli* (Fig. 3C), more pronounced for the 80% material. Although this behaviour was only observed in the experiments with ZnO and *E.coli*, it has previously been reported for both TiO_2- and ZnO-mediated inactivation of *S. aureus* [46]. This initial slow-inactivation time reduces the calculated rate constants and the R^2 values obtained in this specific case. However, ZnO-containing pellets generally showed better disinfection efficiency than their TiO_2 counterparts for both microorganisms (Fig. 3C,D; Table 2), although for the inactivation of *S. aureus* with pellets containing 60% semiconductor, the TiO_2 material proved to be more efficient. Also, as observed for TiO_2, the inactivation of *S. aureus* with ZnO pellets is faster than that of *E. coli*. At this point, it should be noted that the inactivation curve, and therefore the corresponding kinetic constant, measured for the experiment with 10 g·L^{-1} of 60% ZnO composites with *E. coli* is anomalous. This reaction was too slow compared to the treatments with another semiconductor, percentage or load. Therefore, it has not been taken into account in the averages presented in this section.

As already found for TiO_2, the ZnO-composite loading has effect on the disinfection rate, increasing by 30% with twice loading. Higher kinetic constants were again calculated for the tests carried out with 80% ZnO pellets, and this effect is particularly relevant in the case of *S. aureus*, where the times required to achieve a 4 log reduction with this material are half those required with the 60% ZnO composite (Table 2). Higher semiconductor percentage and catalyst loading resulted in higher disinfection rates, with ZnO composites usually showing better disinfection efficacy. Consequently, it was found that inactivation was always faster with 20 g·L^{-1} of 80% ZnO composite.

According to these results, two important points were identified: i) the UVA-mediated photocatalytic inactivation of both bacteria is generally faster with ZnO pellets, indicating that this semiconductor has a higher catalytic activity under the conditions used in the study, despite its *ca.* 0.2 eV higher energy gap (E_g) with respect to TiO_2 [47], ii) the rate constants obtained for *S. aureus* are higher with all the composites used. Numerous studies have evaluated the activity of TiO_2-P25 and ZnO nanoparticles for the photodegradation of chemical pollutants under artificial UVA-Visible radiation. In some experiments ZnO has shown higher absorption range, longer-lived e^-/h^+ pair and much higher e^- mobility as compared to TiO_2 [48]. However, published results indicate different findings: while some research found ZnO to be a more efficient catalyst [49,50], other studies showed faster degradation with TiO_2-P25 [51,52]. Other photocatalytic studies have also examined the UV-photocatalytic disinfection of microorganisms using the same semiconductor catalysts and found that either TiO_2 [44] or ZnO [53,54] can be more efficient. Although the general trend is that gram-negative

Table 2
Kinetic parameters of the inactivation of *E. coli* and *S. aureus* in artificial UVA light tests with TiO_2- and ZnO-clay composite photocatalysts as a function of the percentage of semiconductor and composite loading. Results obtained for single UVA radiation (without any photocatalyst) are also collected. Natural pH, distilled water, T = 30 °C.

Semiconductor	Percentage (%)	Loading ($g \cdot L^{-1}$)	k_{obs} (min^{-1})	S.E.	R^2	4 log Red. (min)
E. coli						
Single UVA			0.014	0.001	0.9852	640
TiO_2	60	10	0.035	0.002	0.9847	262
		20	0.055	0.004	0.9569	167
	80	10	0.047	0.002	0.9851	194
		20	0.083	0.007	0.9571	111
ZnO	60	10	0.028	0.001	0.9913	332
		20	0.075	0.008	0.9232	123
	80	10	0.070	0.009	0.8915	131
		20	0.091	0.022	0.7256	102
S. aureus						
Single UVA			0.018	0.001	0.9794	505
TiO_2	60	10	0.092	0.013	0.9110	100
		20	0.128	0.017	0.9012	72
	80	10	0.132	0.010	0.9716	70
		20	0.147	0.007	0.9847	63
ZnO	60	10	0.082	0.006	0.9768	112
		20	0.095	0.003	0.9933	97
	80	10	0.145	0.011	0.9577	63
		20	0.207	0.001	0.9999	45

bacteria are more easily inactivated than gram-positive bacteria [44,53], some studies show similar behaviour between the photocatalytic inactivation of gram-negative and gram-positive bacteria [55], while others report greater disinfection rates for gram-positive bacteria when compared with gram-negative [56], which is in line with the results obtained in this study.

It is known that the two semiconductors used have some antimicrobial properties through interaction with some molecules present in the bacterial cell wall [44,57]. In fact, the bacterial inactivation routes within photocatalytic disinfection involves both direct contact of the composite with the bacterial cell wall by electrostatic interaction and bacterial damage caused by ROS generated due to the photocatalytic activity of the composites [58]. Dark tests were conducted with the different photocatalysts, resulting in log removal values of 0.85 ± 0.07 and 0.18 ± 0.01 (*S. aureus*) and 0.84 ± 0.91 and 0.11 ± 0.11 (*E. coli*) in 4 h for TiO_2 and ZnO composites, respectively. These values indicate relatively low elimination levels attributed to the direct interaction between the bacterial cells and the macrocomposites or the leached semiconductor particles (either by adsorption or by inactivation due to semiconductor toxicity).

Although the main differences in photocatalytic inactivation are mainly related to differences in cell wall structure and protection mechanisms, the adhesion of bacteria to the surface of the material and the subsequent bacteria-catalyst interaction are important factors affecting the efficiency of photocatalytic water disinfection [54,59]. It has been shown that the ζ-potential controls these non-specific interactions and plays a relevant role in the adsorption processes [60]. Accordingly, depending on the type of bacteria, they would be more attracted to the macrocomposites due to the electrostatic interactions, which depend on both the ζ-potential of the pellets and the bacteria.

In this regard, the ζ-potential of the raw materials, which should be at least partially retained in the pellets produced, is shown in Table 1. Both TiO_2 and ZnO present positive charge at their surface, while P_1M_2 clay has a negative ζ-potential. On the other hand, no significant differences are supposed to appear in isoelectric behaviour of gram-negative and gram-positive bacteria [56,59,60]. However, slightly more negative charges have been reported for gram-negative bacteria [61], in particular the average ζ-potential of *E coli* is approximately 10 mV more negative than that of *S. aureus* [61,62]. This difference probably determines the interaction between bacteria and TiO_2 or ZnO, which can qualitatively explain the faster inactivation rate usually observed for gram-negative species. On the other hand, the presence of the clay with its negative surface charge, even at low concentrations relative to the semiconductors, may alter the ζ-potential of the catalytic material sufficiently to tip the balance towards faster inactivation of *S. aureus*, *i.e.*, the gram-positive species. This could also be the reason for the slightly higher removal of *S. aureus* observed in the dark. In any case, the bactericidal effectiveness can be linked to the photocatalytic properties of the semiconductors: cell compounds can be either reduced or oxidised by e^- or h^+, respectively, on the catalyst surface, or damaged by photogenerated ROS, including hydroxyl radical ($HO^\bullet$), but also superoxide anion or singlet oxygen. These processes, and therefore inactivation, are mostly surface processes, as it has been shown that $HO^\bullet$ migration into the bulk of the solution is highly ineffective, reaching only a few atomic distances from the surface [63], where its concentration is higher [64]. The detailed mechanism of inactivation of *E. coli* and *S. aureus* by $HO^\bullet$ and other photogenerated ROS is beyond the scope of this study. However, bacterial killing by exogenous $HO^\bullet$ has already been studied and the relevant biocidal activity of this radical, which acts by damaging both the cell wall and the cell membrane, has been demonstrated [65–67].

3.3. Solar tests

The results obtained regarding solar experimentation are represented in Fig. 4, where the inactivation profiles of *S. aureus* and *E. coli* are displayed; corresponding kinetic values are listed in Table 3. Again, data measured in the dark are shown for comparison.

Solar inactivation was shown to be much faster than with single UVA irradiation. Sunlight achieved between 2 and 3 log inactivation of both bacteria in only 1 h (Fig. 4), whereas similar inactivation with the UVA lamp required approximately 4 times longer exposure times. Thus, sunlight is more efficient than the 365 nm UVA radiation used, even though the higher radiation intensity measured with the latter. The irradiated area in these flasks is slightly larger (0.6%) than in the quartz tube used in the UVA experiments, but the volume of the solution treated, and therefore the amount of bacteria, is half in the solar tests. Furthermore, in the solar reactor, the entire volume (100 mL) of the contaminated solution was irradiated simultaneously, whereas in the flow reactor only 39 mL out of a total of 200 mL were exposed to UVA radiation. Therefore, the results from the two photoreactors cannot be easily compared. Furthermore, the effects of the two types of radiations

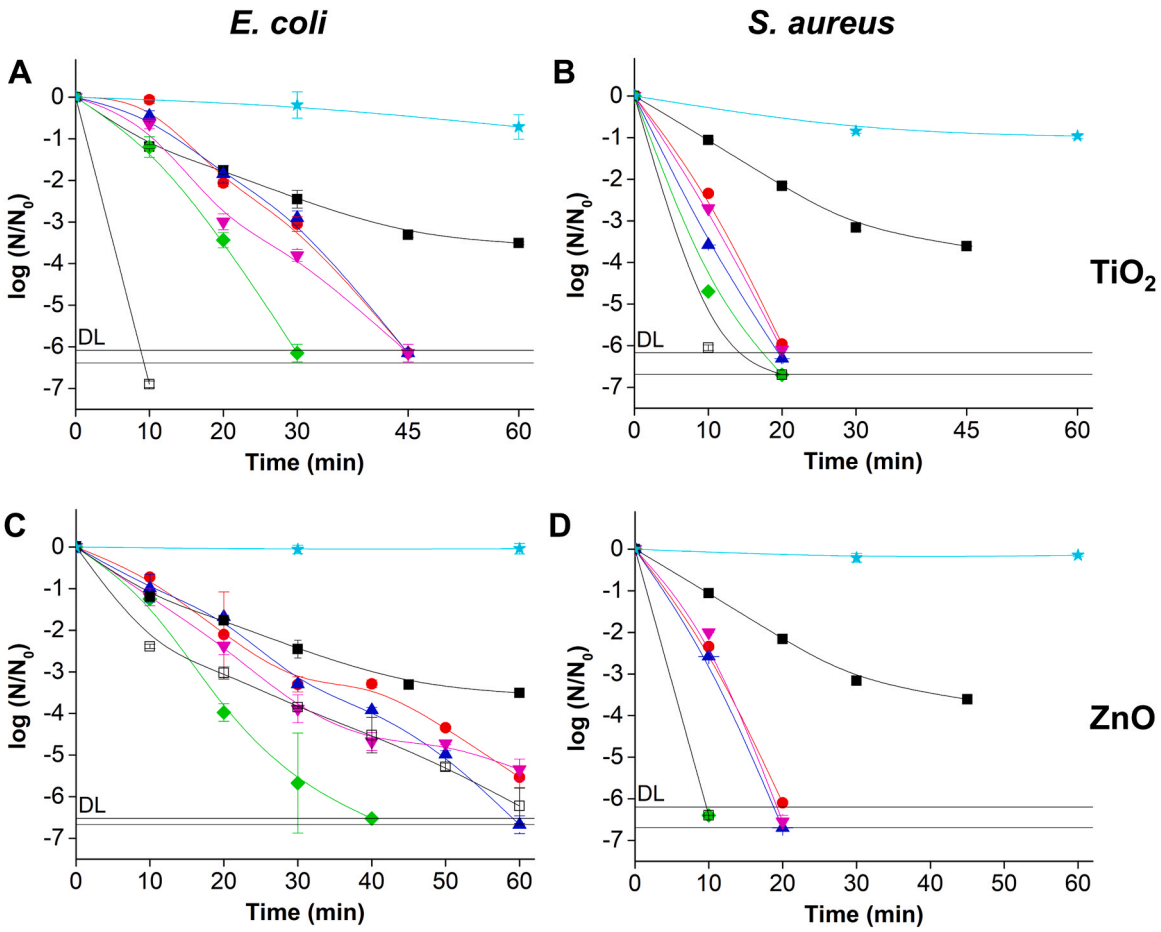

Fig. 4. Solar inactivation of *E. coli* (A, C) and *S. aureus* (B, D) with TiO_2 (A, B) and ZnO (C, D) photocatalysts as a function of composite loading and semiconductor percentage: dark test with 20 g·L^{-1} of 80% pellets (—★—),solar inactivation (—■—), and photocatalysis with 0.5 g·L^{-1} of powdered semiconductor in suspension (—□—) or with 20 g·L^{-1} of 60% (—●—), 20 g·L^{-1} of 80% (—▲—), 40 g·L^{-1} of 60% (—▼—), and 40 g·L^{-1} of 80% (—◆—) pellets. Natural pH, distilled water, T *ca.* 30 °C. Note: (—□—) and (—◆—) profiles are fully coincident in Fig. 4D.

used (artificial UVA and sunlight) on the bacteria and on the semiconductors are quite different.

UVA radiation inactivates bacterial cells mainly due to intracellular mechanisms [43,68]. Sunlight has a broader emission spectrum, including a very small percentage of UVB radiation, which is the major responsible for DNA damage [42,68], although the samples are contained in flasks made of borosilicate glass, which filters some wavelengths in the UVB range very efficiently [69].

The inactivation of both bacteria was again enhanced in the presence of the photocatalytic composites (Fig. 4, Table 3), with rates 1.3–2.5 times that of sunlight exposure for *E.coli*, and 2.3–6.3 times for *S. aureus*; not as much as with the UVA lamp. This difference arises from the fact that virtually all of the lamp radiation ($\lambda = 365$ nm) could promote the electrons from the valence band to the conduction band, resulting in e^-/h^+ pairs and enhancing the catalysed process, whereas solar UV radiation was of lower irradiance, but it has higher disinfection effect than UVA radiation.

As the inactivation rates in the UVA experiments increased with composite loading, and to take advantage of the higher surface area available for pellet placement, loadings of 20 and 40 g·L^{-1} were used in the solar assays. Some similar trends to those observed in the UVA tests were found in these experiments: slightly higher kinetic constants were obtained with increasing semiconductor percentage and composite loading. However, a significant acceleration of the inactivation of both bacterial species was observed when these two variables were fixed at 80% and 40 g·L^{-1}, especially with ZnO. Thus, an increase of approximately 100% in the rate constants was calculated when going from 10 to 20 g·L^{-1} of 80% ZnO catalyst or from 60% to 80% ZnO with 20 g·L^{-1} loading. This effect can also be partially observed with TiO_2 and *E. coli*. As reported with UVA, the inactivation of *S. aureus* was faster than that of *E. coli*, with kinetic constants 90–240% higher for the former.

For comparison, disinfection with particulate TiO_2-P25 and ZnO was also measured. The inactivation curves are shown in Fig. 4 and the rate constants given in Table 3. P25 is very effective against both bacteria, faster than TiO_2 composites developed in this study, but still *S. aureus* is better inactivated with 40 g·L^{-1} of 80% ZnO material. On the other hand, ZnO is also quite effective with *S. aureus*, similar to the best composite, while *E. coli* inactivation is slower than with several types of catalytic pellets.

In contrast to the UVA tests, the general trend observed is that the faster inactivation processes were measured with TiO_2 composites. Nevertheless, the best disinfection was obtained with 40 g·L^{-1} of 80% ZnO pellets: the kinetic constants are very similar for *E. coli* (only a 0.2% increase), but much higher for *S. aureus* (77% faster rate than in the corresponding TiO_2 test). It agrees with most solar photodegradation and photodisinfection studies, which reported that ZnO was found to be more effective under sunlight than TiO_2 [70–72].

In addition, an unusual behaviour is observed for *E. coli*. Its inactivation with TiO_2 and ZnO materials runs parallel during the first 30 min, but then the ZnO-mediated disinfection slows down; such difference

Table 3
Kinetic parameters of the inactivation of *E. coli* and *S. aureus* in solar tests with TiO_2- and ZnO-clay composite photocatalysts as a function of the percentage of semiconductor and composite loading. Results obtained for sunlight exposure (without any photocatalyst) and photocatalysis with powdered semiconductors in suspension are also collected. Natural pH, distilled water, T *ca.* 30 °C.

Semiconductor	Percentage (%)	Loading ($g \cdot L^{-1}$)	k_{obs} (min^{-1})	S.E.	R^2	4 log Red. (min)
E. coli						
Solar inactivation			0.173	0.012	0.9749	53
TiO_2	60	20	0.286	0.028	0.9619	32
		40	0.310	0.016	0.9899	30
	80	20	0.278	0.030	0.9561	33
		40	0.436	0.042	0.9730	21
	100	0.5	$\geq$ 1.589	0.000	1.0000	$\leq$ 6
ZnO	60	20	0.222	0.008	0.9916	42
		40	0.239	0.017	0.9695	39
	80	20	0.247	0.005	0.9968	37
		40	0.437	0.006	0.9993	21
	100	0.5	0.249	0.010	0.9898	37
S. aureus						
Solar inactivation			0.234	0.013	0.9873	39
TiO_2	60	20	0.647	0.065	0.9800	14
		40	0.686	0.032	0.9956	13
	80	20	0.727	0.009	0.9997	13
		40	0.833	0.124	0.9565	11
	100	0.5	1.358	0.142	0.9784	7
ZnO	60	20	0.549	0.041	0.9892	17
		40	0.753	0.012	0.9995	12
	80	20	0.691	0.088	0.9678	13
		40	$\geq$ 1.473	0.000	1.0000	$\leq$ 6
	100	0.5	$\geq$ 1.473	0.000	1.0000	$\leq$ 6

could be related to photoinstability of ZnO materials, which would delay the inactivation reaction. The photocorrosion of ZnO in aqueous solution under UV irradiation is well known [49], but if this had occurred, such a slowdown should have been maintained in subsequent uses of the catalyst, and this was not observed (see Section 3.4). In addition, a similar effect should have occurred with *S. aureus*, although the reaction is so fast that inactivation is always completed in less than 30 min, but this was not observed in the reuses either.

3.4. Applicability

Good catalytic activity is essential for the selection of a photocatalyst, but its potential application in water treatment processes depends on several factors. Nanoparticles have a much higher surface area and therefore catalytic activity, but they also present some important drawbacks, mainly related to their difficult recovery and inherent cytotoxicity. Supported materials facilitate the recovery of the catalyst and their macro nature reduces the cytotoxicity factor, but often catalytic activity is lost when reusing, and a continuous replacement is costly. Therefore, the reuse of photocatalytic material is key for any potential application in water disinfection.

The macrophotocatalysts produced in this study can be easily recovered by simple gravity filtration or even decantation, in a cost-effective manner, as they are placed at the bottom of the reactor. Thus, after the first use, the composites were recovered and used in subsequent experiments (Figs. 5 and 6). In the UVA inactivation assays, the disinfection efficacy was highly conserved and no efficiency loss was observed after up to three uses.

The inactivation kinetics with solar radiation and reused photocatalysts are shown in Fig. 6. Despite an occasional loss of efficacy observed in some experiments, mainly *E. coli* inactivation with TiO_2 materials (Fig. 6A), the composites again retain their photocatalytic activity after three consecutive uses under similar conditions. This is due to the homogeneous structure of the photocatalyst, without any detachable film, which keeps the material active after each use: if one of the photocatalytic pellets is broken, or its surface eroded, a new surface appears with the same composition and activity as the original. We have previously shown that there is no significant leaching from the TiO_2 pellets (and within regulated limits from the ZnO pellets), ensuring their chemical and mechanical stability.

In some of the reuse tests (*e.g.,* Figs. 5A and 6A), substantial rate differences were obtained between successive cycles. This is probably due to the fact that the pellets are not uniformly distributed on the bottom of the reactor and therefore the illuminated area can vary significantly from run to run. Indeed, we observed a similar behaviour in the solar photodegradation of phenol, although we were able to reuse the same TiO_2 pellets for fifteen 7-hour cycles without any appreciable loss of activity (preliminary data not yet published).

Other key factors for the application of these composites in water disinfection would be the toxicity of the treated water and the cost of treatment. No concentration limits for the presence of Ti and Zn in drinking water are established in EU or US EPA regulations [40,41]. However, due to the much higher amount of leached Zn found in the water and the higher photocorrosion resistance of TiO_2, the use of the more stable TiO_2 pellets seems more reasonable. Also, they showed quite good reusability in phenol degradation experiments. The use of sunlight is crucial to achieve an economical and sustainable treatment, and considering the data obtained in the solar experiments with the TiO_2 composites (Table 3), the lower loading (20 $g \cdot L^{-1}$) proves to be more cost effective, as the inactivation rate does not increase proportionally to the loading.

The composition ratio of the composite pellets has an effect on their activity but on their production costs as well. The addition of clay to the pellets, apart from allowing higher calcination temperatures to obtain harder composites [32], subtracts some cost to the production of the material as clays are quite inexpensive. This saving is more relevant when using pellets containing 40% clay, as this difference had little effect on the catalytic activity. In addition, the use of anatase instead of P25 also reduces costs. Thus, a rough estimate of the cost of industrial production of 1 kg of 60% TiO_2 (anatase) pellets could be around €1–1.5. Their use in simple shallow basins for solar water treatment, with at least 15 cycles, corresponds to a low treatment cost of 1.3–2 $€ \cdot m^3$, or probably less, since disinfection is achieved in a shorter time, and without costly facilities or continuous consumption of energy and chemicals. In fact, a similar composite (containing another clay with lower activity) has been tested as a tertiary treatment after a hybrid

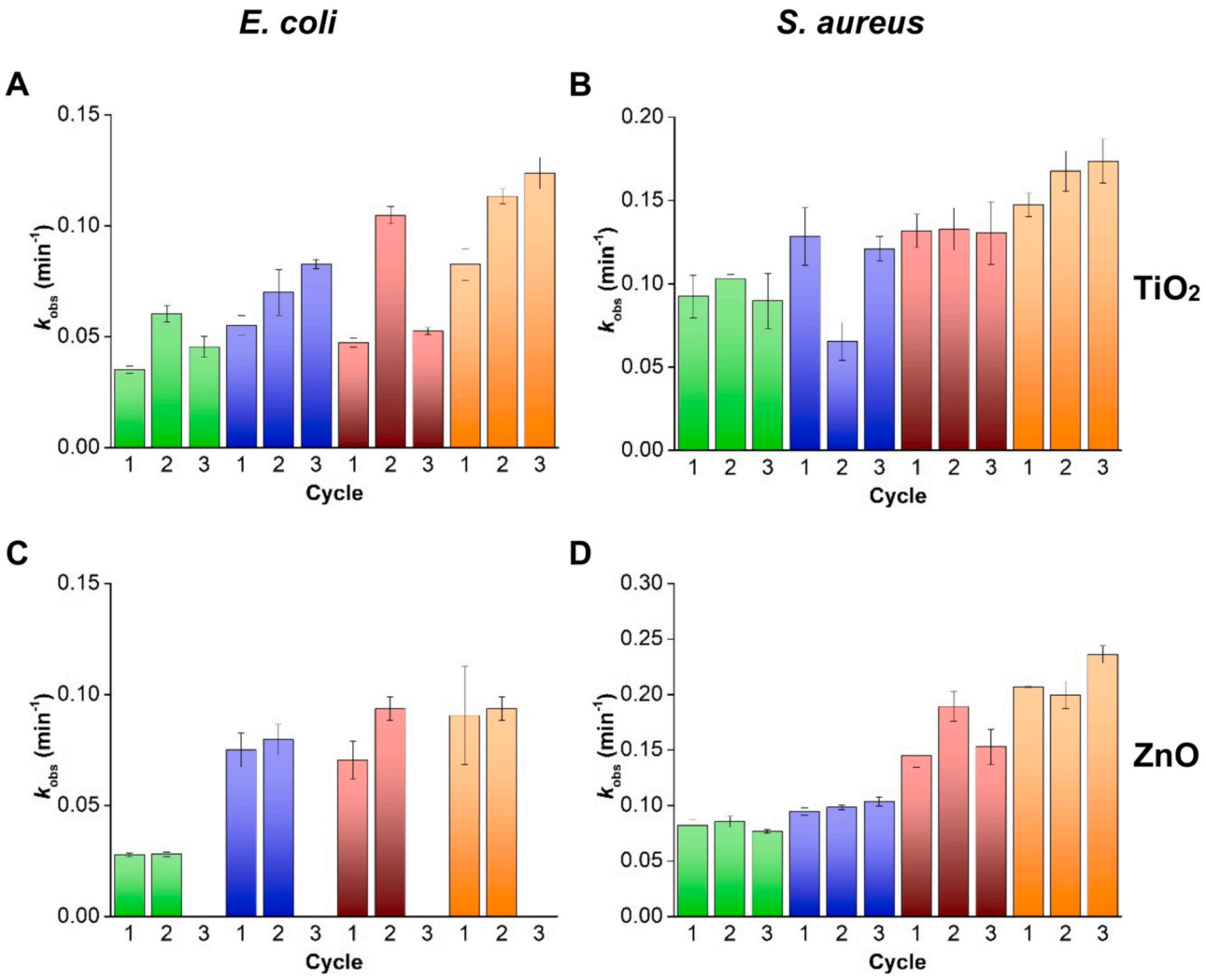

Fig. 5. First order rate constants of *E. coli* and *S. aureus* inactivation with UVA radiation and reused TiO_2 and ZnO photocatalytic materials as a function of composite loading and semiconductor percentage: 10 g·L^{-1} of 60% ( ), 20 g·L^{-1} of 60% ( ), 10 g·L^{-1} of 80% ( ), and 20 g·L^{-1} of 80% ( ) pellets. Natural pH, distilled water, T = 30 °C.

digester and a vertical flow constructed wetland for wastewater treatment. Thus, a bed of 2 kg of photocatalytic pellets was used in a 1 m^2 photoreactor with 50 L of effluent for 2 h under sunlight, with satisfactory removal of several persistent pollutants [33] and pathogens [73].

A number of issues still need to be considered: composite washing between cycles would add some extra cost to the treatment, although the benefits of this cleaning process need to be further investigated; the requirement for large unshaded areas to treat large volumes of water; and the possibility of fouling in long-term use (more than 15 7-hour cycles). However, the photocatalysts used here appear to be a promising option for water treatment and disinfection in small communities with extensive areas of available land.

4. Conclusions

The photocatalytic macrocomposites prepared with Ecuadorian clay and two semiconductors (TiO_2 and ZnO) were successfully tested on the inactivation of two different bacteria: *Staphylococcus aureus* and *Escherichia coli*. These composites showed high disinfection rates with different irradiation sources (sunlight and UVA lamp).

In general, the disinfection efficacy is improved by the presence of both macrocomposites under UVA irradiation, although inactivation is generally faster with ZnO pellets, indicating that this semiconductor has a higher catalytic activity. Higher percentage of semiconductors and catalyst loading resulted in higher disinfection rates, although the disinfection rate does not increase linearly with either composite loading or semiconductor percentage.

A similar behaviour has been obtained when photocatalysts were tested under solar irradiation but with higher disinfection rates. In contrast to the UVA tests, the general trend observed is that the faster inactivation processes were measured with TiO_2 composites. Nevertheless, the highest disinfection rates were obtained with 40 g·L^{-1} of 80% ZnO pellets, with results comparable to those obtained with pure nanosized TiO_2 and ZnO.

In addition, since the photocatalytic material can be easily recycled due to its bulky size, while the bacterial inactivation rate remains constant, the composites proposed in this study could be easily scaled up and have a promising future as water disinfection agents on a larger scale.

CRediT authorship contribution statement

S. Aguilar: Conceptualization, Methodology, Formal analysis,

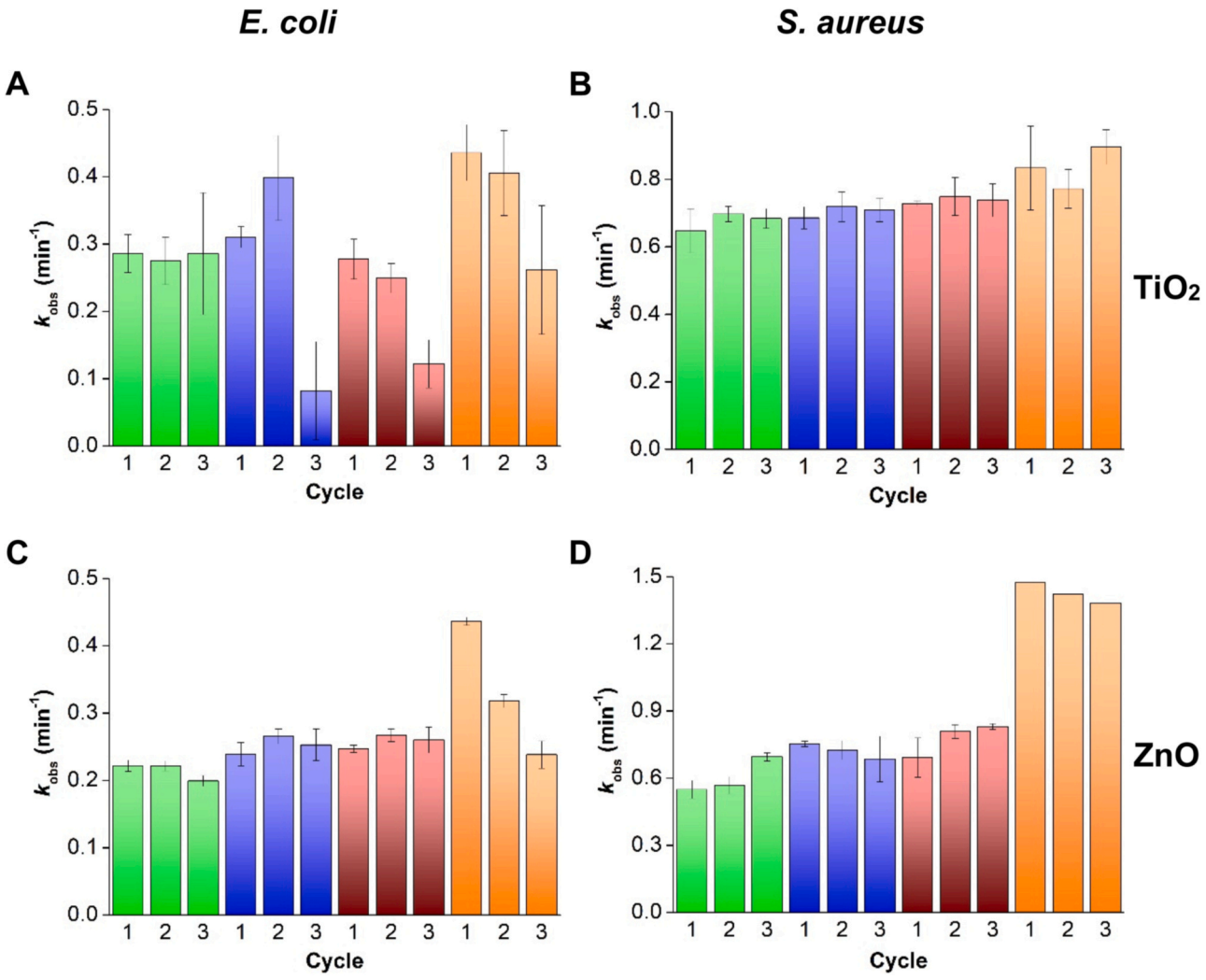

Fig. 6. First order rate constants of *E. coli* and *S. aureus* inactivation with sunlight radiation and reused TiO_2 and ZnO photocatalytic materials as a function of composite loading and semiconductor percentage: 20 g·L^{-1} of 60% ( ), 40 g·L^{-1} of 60% ( ), 20 g·L^{-1} of 80% ( ), and 40 g·L^{-1} of 80% ( ) pellets. Natural pH, distilled water, T *ca.* 30 °C.

Investigation, Writing – original draft, Funding acquisition. **B. Guerrero:** Investigation. **A. Benítez:** Formal analysis, Investigation. **D. R. Ramos:** Formal analysis, Writing – original draft, Writing – review & editing. **J. A. Santaballa:** Writing – review & editing, Funding acquisition. **M. Canle**: Writing – review & editing, Funding acquisition. **D. Rosado:** Formal analysis, Investigation, Writing – original draft. **J. Moreno-Andrés**: Conceptualization, Methodology, Formal analysis, Writing – original draft, Writing – review & editing, Supervision.

Declaration of Competing Interest

The authors declare the following financial interests/personal relationships which may be considered as potential competing interests: Silvio Aguilar has patent #PCT ES2021/070940 pending to Universidade da Coruña & Universidad Técnica Particular de Loja. Daniel R. Ramos has patent #PCT ES2021/070940 pending to Universidade da Coruña & Universidad Técnica Particular de Loja. J. Arturo Santaballa has patent #PCT ES2021/070940 pending to Universidade da Coruña & Universidad Técnica Particular de Loja. Moisés Canle has patent #PCT ES2021/070940 pending to Universidade da Coruña & Universidad Técnica Particular de Loja.

Data Availability

Data will be made available on request.

Acknowledgements

This research has received support from the Spanish Ministerio de Ciencia e Innovación, through grant TED2021–132667B-I00, funded by the EU NextGeneration EU/PRTR through project MCIN/AEI/10.13039/501100011033. Financial support was provided also by the regional government of the *Xunta de Galicia* through project GPC/ED431B 2020/52. S.A. acknowledges the *Universidad Técnica Particular de Loja* for financial support to carry out PhD studies at the Universidade da Coruña, D.R.R thanks the *Universidade da Coruña for a Margarita Salas* contract and J.M.A. acknowledges a grant IJC2020–042741-I funded by MCIN/AEI/10.13039/501100011033 and the European Union NextGenerationEU/PRTR. Funding for open access charge: Universidade da Coruña/CISUG.

References

[1] World Health Organization. Drinking-water key facts. 2019. https://www.who.int/news-room/fact-sheets/detail/drinking-water (Accessed 20 April 2023).

[2] A. Gallego-Schmid, R.R.Z. Tarpani, Life cycle assessment of wastewater treatment in developing countries: a review, Water Res. 153 (2019) 63–79, https://doi.org/10.1016/j.watres.2019.01.010.

[3] World Health Organization; UNICEF. Progress on drinking water, sanitation and hygiene: 2017 update and SDG baselines. 2017. https://apps.who.int/iris/rest/bitstreams/1087296/retrieve (Accessed 20 April 2023).

[4] United Nations. Transforming our world: the 2030 Agenda for Sustainable Development. 2015. https://sdgs.un.org/2030agenda (Accessed 20 April 2023).

[5] B.J.M. Chaúque, M.B. Rott, Solar disinfection (SODIS) technologies as alternative for large-scale public drinking water supply: advances and challenges, Chemosphere 281 (2021), 130754, https://doi.org/10.1016/j.chemosphere.2021.130754.

[6] J. Moreno-SanSegundo, S. Giannakis, S. Samoili, G. Farinelli, K.G. McGuigan, C. Pulgarín, J. Marugán, SODIS potential: a novel parameter to assess the suitability of solar water disinfection worldwide, Chem. Eng. J. 419 (2021), 129889, https://doi.org/10.1016/j.cej.2021.129889.

[7] G. Boczkaj, A. Fernandes, Wastewater treatment by means of advanced oxidation processes at basic pH conditions: a review, Chem. Eng. J. 320 (2017) 608–633, https://doi.org/10.1016/j.cej.2017.03.084.

[8] S. Malato, P. Fernández-Ibáñez, M.I. Maldonado, J. Blanco, W. Gernjak, Decontamination and disinfection of water by solar photocatalysis: recent overview and trends, Catal. Today 147 (2009) 1–59, https://doi.org/10.1016/j.cattod.2009.06.018.

[9] Y. Aguas, M. Hincapie, P. Fernández-Ibáñez, M.I. Polo-López, Solar photocatalytic disinfection of agricultural pathogenic fungi (*Curvularia* sp.) in real urban wastewater, Sci. Total Environ. 607–608 (2017) 1213–1224, https://doi.org/10.1016/j.scitotenv.2017.07.085.

[10] I. Jeon, E.C. Ryberg, P.J.J. Alvarez, J.H. Kim, Technology assessment of solar disinfection for drinking water treatment, Nat. Sustain. 5 (2022) 801–808, https://doi.org/10.1038/s41893-022-00915-7.

[11] C. Li, N. Zhu, S. Yang, X. He, S. Zheng, Z. Sun, D.D. Dionysiou, A review of clay based photocatalysts: role of phyllosilicate mineral in interfacial assembly, microstructure control and performance regulation, Chemosphere 273 (2021), 129723, https://doi.org/10.1016/j.chemosphere.2021.129723.

[12] W.J. Ong, L.L. Tan, Y.H. Ng, S.T. Yong, S.P. Chai, Graphitic cabon nitride ($g\text{-}C_3N_4$)-based photocatalysts for artificial photosynthesis and environmental remediation: are we a step closer to achieving sustainability? Chem. Rev. 116 (2016) 7159–7329, https://doi.org/10.1021/acs.chemrev.6b00075.

[13] M.C. Dlamini, M.S. Maubane-Nkadimeng, J.A. Moma, The use of TiO_2/clay heterostructures in the photocatalytic remediation of water containing organic pollutants: a review, J. Environ. Chem. Eng. 9 (2021), 106546, https://doi.org/10.1016/J.JECE.2021.106546.

[14] O.H. Aremu, C.O. Akintayo, E.B. Naidoo, S.M. Nelana, O.S. Ayanda, Synthesis and applications of nano-sized zinc oxide in wastewater treatment: a review, Int. J. Environ. Sci. Technol. 18 (2021) 3237–3256, https://doi.org/10.1007/s13762-020-03069-1.

[15] Y. Liang, W. Li, X. Wang, R. Zhou, H. Ding, TiO_2–ZnO/Au ternary heterojunction nanocomposite: excellent antibacterial property and visible-light photocatalytic hydrogen production efficiency, Ceram. Int. 48 (2022) 2826–2832, https://doi.org/10.1016/j.ceramint.2021.10.072.

[16] J. Liu, Y. Wang, J. Ma, Y. Peng, A. Wang, A review on bidirectional analogies between the photocatalysis and antibacterial properties of ZnO, *J. Alloy. Compd.* 783 (2019) 898–918, https://doi.org/10.1016/j.jallcom.2018.12.330.

[17] K. Siwińska-Stefańska, A. Kubiak, A. Piasecki, A. Dobrowolska, K. Czaczyk, M. Motylenko, D. Rafaja, H. Ehrlich, T. Jesionowski, Hydrothermal synthesis of multifunctional TiO_2-ZnO oxide systems with desired antibacterial and photocatalytic properties, Appl. Surf. Sci. 463 (2019) 791–801, https://doi.org/10.1016/J.APSUSC.2018.08.256.

[18] S.K. Loeb, P.J.J. Alvarez, J.A. Brame, E.L. Cates, W. Choi, J. Crittenden, D. D. Dionysiou, Q. Li, G. Li-Puma, X. Quan, et al., The technology horizon for photocatalytic water treatment: sunrise or sunset? Environ. Sci. Technol. 53 (2019) 2937–2947, https://doi.org/10.1021/acs.est.8b05041.

[19] G. Lofrano, M. Carotenuto, G. Libralato, R.F. Domingos, A. Markus, L. Dini, R. K. Gautam, D. Baldantoni, M. Rossi, S.K. Sharma, et al., Polymer functionalized nanocomposites for metals removal from water and wastewater: an overview, Water Res. 92 (2016) 22–37, https://doi.org/10.1016/J.WATRES.2016.01.033.

[20] V. Parvulescu, M. Ciobanu, G. Petcu, Immobilization of semiconductor photocatalysts, Handb. Smart Photo Mater. (2020) 103–140, https://doi.org/10.1016/b978-0-12-819051-7.00004-x.

[21] N.U. Saqib, R. Adnan, I. Shah, M. Arshad, M. Inam, Activated carbon, zeolite, and ceramics immobilized TiO_2 photocatalysts for the enhanced sequential uptake of dyes and Cd^{2+} ions, J. Dispers. Sci. Technol. (2022) 2070497, https://doi.org/10.1080/01932691.2022.2070497.

[22] A. Bouarioua, M. Zerdaoui, Photocatalytic activities of TiO_2 layers immobilized on glass substrates by dip-coating technique toward the decolorization of methyl orange as a model organic pollutant, *J. Environ. Chem. Eng.* 5 (2017) 1565–1574, https://doi.org/10.1016/j.jece.2017.02.025.

[23] L. Yang, F. Wang, A. Hakki, D.E. Macphee, P. Liu, S. Hu, The influence of zeolites fly ash bead/TiO_2 composite material surface morphologies on their adsorption and photocatalytic performance, Appl. Surf. Sci. 392 (2017) 687–696, https://doi.org/10.1016/j.apsusc.2016.09.023.

[24] S. Razak, M.A. Nawi, K. Haitham, Fabrication, characterization and application of a reusable immobilized TiO_2-PANI photocatalyst plate for the removal of reactive red 4 dye, Appl. Surf. Sci. 319 (2014) 90–98, https://doi.org/10.1016/j.apsusc.2014.07.049.

[25] D.R. Ramos, M. Iazykov, M.I. Fernandez, J.A. Santaballa, M. Canle, Mechanical stability is key for large-scale implementation of photocatalytic surface-attached film technologies in water treatment, Front. Chem. Eng. 3 (2021), 688498, https://doi.org/10.3389/fceng.2021.688498.

[26] S. Teixeira, P.M. Martins, S. Lanceros-Méndez, K. Kühn, G. Cuniberti, Reusability of photocatalytic TiO_2 and ZnO nanoparticles immobilized in poly(vinylidene difluoride)-co-trifluoroethylene, Appl. Surf. Sci. 384 (2016) 497–504, https://doi.org/10.1016/j.apsusc.2016.05.073.

[27] H. Bel Hadjltaief, M. Ben Zina, M.E. Galvez, P. Da Costa, Photocatalytic degradation of methyl green dye in aqueous solution over natural clay-supported ZnO-TiO_2 catalysts, J. Photochem. Photobiol. A-Chem. 315 (2016) 25–33, https://doi.org/10.1016/j.jphotochem.2015.09.008.

[28] S. Mustapha, M.M. Ndamitso, A.S. Abdulkareem, J.O. Tijani, D.T. Shuaib, A. O. Ajala, A.K. Mohammed, Application of TiO_2 and ZnO nanoparticles immobilized on clay in wastewater treatment: a review, Appl. Water Sci. 10 (2020) 49, https://doi.org/10.1007/S13201-019-1138-Y.

[29] H. Rabah, K. Khaldi, A. Choukchou-Braham, D. Lerari-Zinai, K. Bachari, Comparative study of natural and synthetic clays used as supported catalysts in dyes degradation by advanced oxidation processes. In Advances in Science, in: A. Kallel, M. Ksibi, H. Ben Dhia, N. Khélifi (Eds.), Technology & Innovation, Springer, 2018, pp. 219–222, https://doi.org/10.1007/978-3-319-70548-4_71.

[30] A. Amritha, M. Sundararajan, R.G. Rejith, M.A. Mohammed-Aslam, La-Ce doped TiO_2 nanocrystals: a review on synthesis, characterization and photocatalytic activity, SN Appl. Sci. 1 (2019) 1441, https://doi.org/10.1007/s42452-019-1455-7.

[31] X. Jaramillo-Fierro, S. González, H.A. Jaramillo, F. Medina, Synthesis of the $ZnTiO_3/TiO_2$ nanocomposite supported in ecuadorian clays for the adsorption and photocatalytic removal of methylene blue dye, Nanomaterials 10 (2020) 1891, https://doi.org/10.3390/nano10091891.

[32] S.D. Aguilar, D.R. Ramos, J.A. Santaballa, M. Canle, Preparation, characterization and testing of a bulky non-supported photocatalyst for water pollution abatement, Catal. Today 413–415 (2023), 113992, https://doi.org/10.1016/j.cattod.2022.12.023.

[33] M. Sánchez, D.R. Ramos, M.I. Fernández, S. Aguilar, I. Ruiz, M. Canle, M. Soto, Removal of emerging pollutants by a 3-step system: hybrid digester, vertical flow constructed wetland and photodegradation post-treatments, Sci. Total Environ. 842 (2022), 156750, https://doi.org/10.1016/j.scitotenv.2022.156750.

[34] M. Baruah, S.L. Ezung, A. Supong, P.C. Bhomick, S. Kumar, D. Sinha, Synthesis, characterization of novel Fe-doped TiO_2 activated carbon nanocomposite towards photocatalytic degradation of Congo red, *E. coli*, and *S. aureus*, Korean J. Chem. Eng. 38 (2021) 1277–1290, https://doi.org/10.1007/S11814-021-0830-4.

[35] S. Rtimi, D.D. Dionysiou, S.C. Pillai, J. Kiwi, Advances in catalytic/photocatalytic bacterial inactivation by nano Ag and Cu coated surfaces and medical devices, Appl. Catal. B-Environ. 240 (2019) 291–318, https://doi.org/10.1016/J.APCATB.2018.07.025.

[36] M.T. Taghizadeh, V. Siyahi, H. Ashassi-Sorkhabi, G. Zarrini, ZnO, AgCl and AgCl/ZnO nanocomposites incorporated chitosan in the form of hydrogel beads for photocatalytic degradation of MB, *E. coli* and *S. aureus*, Int. J. Biol. Macromol. 147 (2020) 1018–1028, https://doi.org/10.1016/J.IJBIOMAC.2019.10.070.

[37] X.G. Zhang, D.L. Guan, C.G. Niu, Z. Cao, C. Liang, N. Tang, L. Zhang, X.J. Wen, G. M. Zeng, Constructing magnetic and high-efficiency AgI/$CuFe_2O_4$ photocatalysts for inactivation of *Escherichia coli* and *Staphylococcus aureus* under visible light: inactivation performance and mechanism analysis, Sci. Total Environ. 668 (2019) 730–742, https://doi.org/10.1016/J.SCITOTENV.2019.03.068.

[38] N.H. Kim, H.W. Kim, H. Moon, M.S. Rhee, Sodium chloride significantly enhances the bactericidal actions of carvacrol and thymol against the halotolerant species *Escherichia coli* O157:H7, *Listeria monocytogenes*, and *Staphylococcus aureus*, LWT-Food Sci. Technol. 122 (2020), 109015, https://doi.org/10.1016/j.lwt.2020.109015.

[39] N. Yossa, G. Arce, J. Smiley, M.-C. Jo Huang, L. Yin, R. Bell, S. Tallent, E. Brown, T. Hammack, Survival and detection of *Bacillus cereus* in the presence of *Escherichia coli*, *Salmonella enteritidis*, *Staphylococcus aureus*, *Pseudomonas aeruginosa* and *Candida albicans* after rechallenge in make-up removers, Int. J. Cosmet. Sci. 40 (2018) 67–74, https://doi.org/10.1111/ics.12434.

[40] European Union. Directive (EU), 2020/2184 of the European Parliament and of the Council of 16 December 2020 on the quality of water intended for human consumption, J. Eur. Union 435/1 (2020) 1–62.

[41] US Environmental Protection Agency, National Primary Drinking Water Regulations. 2023. https://www.epa.gov/ground-water-and-drinking-water/national-primary-drinking-water-regulations (Accessed on 3 August 2023).

[42] S. Giannakis, M.I. Polo López, D. Spuhler, J.A. Sánchez Pérez, P. Fernández Ibáñez, C. Pulgarin, Solar disinfection is an augmentable, *in situ*-generated photo-Fenton reaction-Part 1: A review of the mechanisms and the fundamental aspects of the process, *Appl. Catal. B-Environ.* 199 (2016) 199–223, https://doi.org/10.1016/j.apcatb.2016.06.009.

[43] S. Giannakis, A. Gupta, C. Pulgarin, J. Imlay, Identifying the mediators of intracellular *E. coli* inactivation under UVA light: the (photo) Fenton process and singlet oxygen, Water Res. 221 (2022), 118740, https://doi.org/10.1016/j.watres.2022.118740.

[44] R.J. Barnes, R. Molina, J. Xu, P.J. Dobson, I.P. Thompson, Comparison of TiO_2 and ZnO nanoparticles for photocatalytic degradation of methylene blue and the correlated inactivation of gram-positive and gram-negative bacteria, J. Nanopart. Res. 15 (2013) 1432, https://doi.org/10.1007/s11051-013-1432-9.

[45] J. Rodríguez-Chueca, T. Silva, J.R. Fernandes, M.S. Lucas, G.L. Puma, J.A. Peres, A. Sampaio, Inactivation of pathogenic microorganisms in freshwater using HSO_5^-/

UV-A LED and HSO_5^-/M^{n+}/UV-A LED oxidation processes, Water Res. 123 (2017) 113–123, https://doi.org/10.1016/j.watres.2017.06.021.
[46] O. Seven, B. Dindar, S. Aydemir, D. Metin, M.A. Ozinel, S. Icli, Solar photocatalytic disinfection of a group of bacteria and fungi aqueous suspensions with TiO_2, ZnO and Sahara desert dust, J. Photochem. Photobiol. A-Chem. 165 (2004) 103–107, https://doi.org/10.1016/j.jphotochem.2004.03.005.
[47] C. Martínez, M. Canle L, M.I. Fernández, J.A. Santaballa, J. Faria, Kinetics and mechanism of aqueous degradation of carbamazepine by heterogeneous photocatalysis using nanocrystalline TiO_2, ZnO and multi-walled carbon nanotubes–anatase composites, Appl. Catal. B-Environ. 102 (2011) 563–571, https://doi.org/10.1016/j.apcatb.2010.12.039.
[48] Q. Zhang, C.S. Dandeneau, X. Zhou, G. Cao, ZnO nanostructures for dye-sensitized solar cells, Adv. Mater. 21 (2009) 4087–4108, https://doi.org/10.1002/adma.200803827.
[49] Y. Li, W. Xie, X. Hu, G. Shen, X. Zhou, Y. Xiang, X. Zhao, P. Fang, Comparison of dye photodegradation and its coupling with light-to-electricity conversion over TiO_2 and ZnO, Langmuir 26 (2010) 591–597, https://doi.org/10.1021/la902117c.
[50] C. Lizama, J. Freer, J. Baeza, H.D. Mansilla, Optimized photodegradation of Reactive Blue 19 on TiO_2 and ZnO suspensions, Catal. Today 76 (2002) 235–246, https://doi.org/10.1016/S0920-5861(02)00222-5.
[51] M. Qamar, M. Muneer, A comparative photocatalytic activity of titanium dioxide and zinc oxide by investigating the degradation of vanillin, *Desalination* 249 (2009) 535–540, https://doi.org/10.1016/j.desal.2009.01.022.
[52] R.P. Souza, T.K.F.S. Freitas, F.S. Domingues, O. Pezoti, E. Ambrosio, A.M. Ferrari-Lima, J.C. Garcia, Photocatalytic activity of TiO_2, ZnO and Nb_2O_5 applied to degradation of textile wastewater, *J. Photochem. Photobiol. A-Chem.* 329 (2016) 9–17, https://doi.org/10.1016/j.jphotochem.2016.06.013.
[53] H.-L. Liu, T.C.K. Yang, Photocatalytic inactivation of *Escherichia coli* and *Lactobacillus helveticus* by ZnO and TiO_2 activated with ultraviolet light, Process Biochem. 39 (2003) 475–481, https://doi.org/10.1016/S0032-9592(03)00084-0.
[54] J. Moreno-Andrés, J.J. Rueda-Márquez, T. Homola, J. Vielma, M.Á. Moríñigo, A. Mikola, M. Sillanpää, A. Acevedo-Merino, E. Nebot, I. Levchuk, A comparison of photolytic, photochemical and photocatalytic processes for disinfection of recirculation aquaculture systems (RAS) streams, Water Res. 181 (2020), 115928, https://doi.org/10.1016/j.watres.2020.115928.
[55] R. van Grieken, J. Marugán, C. Pablos, L. Furones, A. López, Comparison between the photocatalytic inactivation of Gram-positive *E. faecalis* and Gram-negative *E. coli* faecal contamination indicator microorganisms, Appl. Catal. B-Environ. 100 (2010) 212–220, https://doi.org/10.1016/j.apcatb.2010.07.034.
[56] J. He, Z. Zheng, I.M.C. Lo, Different responses of gram-negative and gram-positive bacteria to photocatalytic disinfection using solar-light-driven magnetic TiO_2-based material, and disinfection of real sewage, Water Res. 207 (2021), 117816, https://doi.org/10.1016/j.watres.2021.117816.
[57] Y.H. Leung, X. Xu, A.P.Y. Ma, F. Liu, A.M.C. Ng, Z. Shen, L.A. Gethings, M.Y. Guo, A.B. Djurišić, P.K.H. Lee, et al., Toxicity of ZnO and TiO_2 to *Escherichia coli* cells, Sci. Rep. 6 (2016) 35243, https://doi.org/10.1038/srep35243.
[58] P. Ganguly, C. Byrne, A. Breen, S.C. Pillai, Antimicrobial activity of photocatalysts: fundamentals, mechanisms, kinetics and recent advances, Appl. Catal. B-Environ. 225 (2018) 51–75, https://doi.org/10.1016/j.apcatb.2017.11.018.
[59] C. Pablos, R. van Grieken, J. Marugán, I. Chowdhury, S.L. Walker, Study of bacterial adhesion onto immobilized TiO_2: effect on the photocatalytic activity for disinfection applications, Catal. Today 209 (2013) 140–146, https://doi.org/10.1016/j.cattod.2012.12.010.
[60] W. Pajerski, D. Ochonska, M. Brzychczy-Wloch, P. Indyka, M. Jarosz, M. Golda-Cepa, Z. Sojka, A. Kotarba, Attachment efficiency of gold nanoparticles by Gram-positive and Gram-negative bacterial strains governed by surface charges, J. Nanopart. Res. 21 (2019) 186, https://doi.org/10.1007/s11051-019-4617-z.
[61] M. Arakha, M. Saleem, B.C. Mallick, S. Jha, The effects of interfacial potential on antimicrobial propensity of ZnO nanoparticle, Sci. Rep. 5 (2015) 9578, https://doi.org/10.1038/srep09578.
[62] S. Halder, K.K. Yadav, R. Sarkar, S. Mukherjee, P. Saha, S. Haldar, S. Karmakar, T. Sen, Alteration of Zeta potential and membrane permeability in bacteria: a study with cationic agents, SpringerPlus 4 (2015) 672, https://doi.org/10.1186/s40064-015-1476-7.
[63] M. Canle L, J.A. Santaballa, E. Vulliet, On the mechanism of TiO_2-photocatalyzed degradation of aniline derivatives, J. Photochem. Photobiol. A-Chem. 175 (2005) 192–200, https://doi.org/10.1016/j.jphotochem.2005.05.001.
[64] S. Zhang, M. Sun, T. Hedtke, A. Deshmukh, X. Zhou, S. Weon, M. Elimelech, J.-H. Kim, Mechanism of heterogeneous Fenton reaction kinetics enhancement under nanoscale spatial confinement, Environ. Sci. Technol. 54 (2020) 10868–10875, https://doi.org/10.1021/acs.est.0c02192.
[65] M. Cho, H. Chung, W. Choi, J. Yoon, Linear correlation between inactivation of *E. coli* and OH radical concentration in TiO_2 photocatalytic disinfection, Water Res. 38 (2004) 1069–1077, https://doi.org/10.1016/j.watres.2003.10.029.
[66] J. Marugán, R. van Grieken, C. Pablos, C. Sordo, Analogies and differences between photocatalytic oxidation of chemicals and photocatalytic inactivation of microorganisms, Water Res. 44 (2010) 789–796, https://doi.org/10.1016/j.watres.2009.10.022.
[67] Y. Hou, X. Li, Q. Zhao, G. Chen, C.L. Raston, Role of hydroxyl radicals and mechanism of *Escherichia coli* inactivation on Ag/AgBr/TiO_2 nanotube array electrode under visible light irradiation, Environ. Sci. Technol. 46 (2012) 4042–4050, https://doi.org/10.1021/es204079d.
[68] T.P. Coohill, J.-L. Sagripanti, Bacterial inactivation by solar ultraviolet radiation compared with sensitivity to 254 nm radiation, Photochem. Photobio. 85 (2009) 1043–1052, https://doi.org/10.1111/j.1751-1097.2009.00586.x.
[69] F.H. ElBatal, M.S. Selim, S.Y. Marzouk, M.A. Azooz, UV–vis absorption of the transition metal-doped SiO_2–B_2O_3–Na_2O glasses, Phys. B 398 (2007) 126–134, https://doi.org/10.1016/j.physb.2007.05.004.
[70] G. Malekshoar, K. Pal, Q. He, A. Yu, A.K. Ray, Enhanced solar photocatalytic degradation of phenol with coupled graphene-based titanium dioxide and zinc oxide, Ind. Eng. Chem. Res. 53 (2014) 18824–18832, https://doi.org/10.1021/ie501673v.
[71] S. Sakthivel, B. Neppolian, M.V. Shankar, B. Arabindoo, M. Palanichamy, V. Murugesan, Solar photocatalytic degradation of azo dye: comparison of photocatalytic efficiency of ZnO and TiO_2, Sol. Energy Mater. Sol. Cells 77 (2003) 65–82, https://doi.org/10.1016/S0927-0248(02)00255-6.
[72] J. Mac Mahon, S.C. Pillai, J.M. Kelly, L.W. Gill, Solar photocatalytic disinfection of *E. coli* and bacteriophages MS2, ΦX174 and PR772 using TiO_2, ZnO and ruthenium based complexes in a continuous flow system, *J. Photochem. Photobiol. B-Biol.* 170 (2017) 79–90, https://doi.org/10.1016/j.jphotobiol.2017.03.027.
[73] Sánchez, M. (PhD thesis). Sistema combinado dixestor-humidal seguido de fotodegradación depuración para a depuración de augas residuais e contaminantes orgánicos emerxentes. Universidade da Coruña, A Coruña, Spain, 2021. http://hdl.handle.net/2183/29365 (Accessed 27 July 2023).